Published OnlineFirst June 2, 2017; DOI: 10.1158/1940-6207.CAPR-17-0010

Research Article

Cancer Prevention Research

# Pigs, Unlike Mice, Have Two Distinct Colonic Stem Cell Populations Similar to Humans That Respond to High-Calorie Diet prior to Insulin Resistance

Venkata Charepalli[1], Lavanya Reddivari[2], Sridhar Radhakrishnan[1], Elisabeth Eriksson[3], Xia Xiao[4], Sung Woo Kim[5], Frank Shen[6], Matam Vijay-Kumar[4,7], Qunhua Li[6], Vadiraja B. Bhat[8], Rob Knight[9,10], and Jairam K.P. Vanamala[1,11,12]

## Abstract

Basal colonic crypt stem cells are long lived and play a role in colon homeostasis. Previous evidence has shown that high-calorie diet (HCD) enhances colonic stem cell numbers and expansion of the proliferative zone, an important biomarker for colon cancer. However, it is not clear how HCD drives dysregulation of colon stem cell/colonocyte proliferative kinetics. We used a human-relevant pig model and developed an immunofluorescence technique to detect and quantify colonic stem cells. Pigs ($n = 8$/group) were provided either standard diet (SD; 5% fat) or HCD (23% fat) for 13 weeks. HCD- and SD-consuming pigs had similar total calorie intake, serum iron, insulin, and glucose levels. However, HCD elevated both colonic proliferative zone (KI-67) and stem cell zone (ASCL-2 and BMI-1). Proliferative zone correlated with elevated innate colonic inflammatory markers TLR-4, NF-κB, IL6, and lipocalin-2 ($r \geq 0.62$, $P = 0.02$). Elevated gut bacterial phyla proteobacteria and firmicutes in HCD-consuming pigs correlated with proliferative and stem cell zone. Colonic proteome data revealed the upregulation of proteins involved in cell migration and proliferation and correlated with proliferative and stem cell zone expansion. Our study suggests that pig colon, unlike mice, has two distinct stem cells (ASCL-2 and BMI-1) similar to humans, and HCD increases expansion of colonic proliferative and stem cell zone. Thus, pig model can aid in the development of preventive strategies against gut bacterial dysbiosis and inflammation-promoted diseases, such as colon cancer. *Cancer Prev Res; 10(8); 1–9. ©2017 AACR.*

## Introduction

The colon is responsible for absorption of water, minerals, and maintaining an immune tolerant symbiotic relationship with the commensal bacteria. As a result, the epithelial cell lining of the colon is under constant exposure to the luminal contents, resulting in a remarkably high rate of cell death, with up to $10^{11}$ epithelial cells (~200 g) being lost every day in humans (1). This high rate of cell death requires continuous and rapid replacement of the cells, which is driven by small populations of long-lived adult stem cells that reside in specialized niches. These stem cells reside in the bottom of the crypt away from the luminal contents. Recent evidence suggests that dysregulation of colon stem cell kinetics not only leads to gut permeability but also colon cancer (2).

Chronic inflammation generates reactive chemical entities (e.g., reactive oxygen, nitrogen, and halogen species) to neutralize invading pathogens, which may also impose chemical damage on nucleic acids and proteins in surrounding cells (3, 4). Prolonged chronic inflammation over a long period, such as in a high-calorie diet (HCD) scenario, may result in chemical damage that exceeds the repair capabilities of the exposed cells, leading to cell death or genetic and epigenetic modifications and the possibility of oncogenic transformation (4). In this context, it is noteworthy that these colonic stem cells play an essential role in maintaining tissue homeostasis and wound repair in the colon by their capacity to self-renew and differentiate to replace the injured cells that die from inflammation and/or injury (5). The same properties also make stem cells prime candidates for accumulating mutations that can result in their transformation to oncogenic stem cells.

Emerging evidence suggests that HCD has a causal link to colon cancer and type II diabetes (6, 7). Prolonged consumption of HCD results in alterations of gut microbiome (8), low-grade colonic, and systemic inflammation/oxidative stress (9, 10).

[1]Department of Food Science, The Pennsylvania State University, University Park, Pennsylvania. [2]Department of Plant Science, The Pennsylvania State University, University Park, Pennsylvania. [3]Biotechnology, Applied Nutrition and Food Chemistry, Lund University, Lund, Sweden. [4]Department of Nutritional Sciences, The Pennsylvania State University, University Park, Pennsylvania. [5]Department of Animal Science, North Carolina State University, Raleigh, North Carolina. [6]Department of Statistics, The Pennsylvania State University, University Park, Pennsylvania. [7]Department of Medicine, The Pennsylvania State University Medical Center, Hershey, Pennsylvania. [8]Agilent Technologies, Wilmington, Delaware. [9]Department of Pediatrics, University of California, San Diego, California. [10]Department of Computer Science and Engineering, University of California, La Jolla, California. [11]The Penn State Hershey Cancer Institute, Hershey, Pennsylvania. [12]Center for Molecular Immunology and Infectious Diseases, The Pennsylvania State University, University Park, Pennsylvania.

**Note:** Supplementary data for this article are available at Cancer Prevention Research Online (http://cancerprevres.aacrjournals.org/).

V. Charepalli and L. Reddivari contributed equally to this article.

Current address for S. Radhakrishnan: Research Diets Inc., New Brunswick, NJ.

**Corresponding Author:** Jairam K.P. Vanamala, Department of Food Science, The Pennsylvania State University, 326 Food Science Building, University Park, PA 16802. Phone: 814-865-6482; Fax: 814-863-6132; E-mail: juv4@psu.edu

**doi:** 10.1158/1940-6207.CAPR-17-0010

©2017 American Association for Cancer Research.



Downloaded from cancerpreventionresearch.aacrjournals.org on October 19, 2017. © 2017 American Association for Cancer Research.

Published OnlineFirst June 2, 2017; DOI: 10.1158/1940-6207.CAPR-17-0010



These factors may contribute to enhanced intestinal permeability, insulin resistance, glucose intolerance (11), and hypoferremia, ultimately leading to elevated risk for colon cancer and type II diabetes. Dysregulation of intestinal stem cell kinetics plays a critical role in colon carcinogenesis; however, it is not clear which of these factors drive the dysregulation, leading to elevated proliferative zone, a well-established risk factor for colon cancer.

There are a wide variety of markers available for the identification of colonic stem cells in murine models, such as ASCL-2 (12), BMI-1 (13), and LGR5 (14). ASCL-2 has been shown to identify stem cells associated with homeostatic regeneration, whereas BMI-1 marks quiescent stem cells that proliferate only during extreme stress/injury to the colonic epithelium (15). In this study, we optimized ASCL-2 and BMI-1 stem cell markers and KI-67 proliferation marker for use on pig colonic tissue to evaluate the colonic stem cell and epithelial cell kinetics using immunofluorescence.

To better understand molecular mechanisms of HCD-altered colonic epithelial kinetics, we utilized functional proteomic studies. Alterations at the protein level can reflect cellular changes more accurately. Advances in bioinformatics and high-throughput technologies have provided powerful tools for unraveling the proteomic profile to identify mechanisms of action of dietary components. As there is no information available on human-relevant pig colon mucosal proteomics, we developed a high-throughput nontargeted, ion-thermal focusing electrospray AJS-ESI LC-MS/MS (Jet Stream Proteomics) approach to identify colon mucosal proteins directly. In addition, the aim of this study was to use proteomics to identify the protein pathways that associate with the changes in the proliferative and stem cell zone in the pig colon.

## Materials and Methods

### Diet-induced inflammation

For the study (Fig. 1A), male pigs (6 weeks old, breed: SPG) were obtained from Murphy-Brown LLC and housed individually in solid indoor pens at the North Carolina State University Swine Educational Unit (Clayton, NC). The animals were divided into different treatment groups by body weight, so that mean initial body weight was similar between the treatment groups ($n = 8$ animals/treatment). Given the number of animals per treatment or sample size being $n = 8$, we only used male pigs as the hormonal changes involved with female pigs would add additional variables that can confound the parameters measured in the

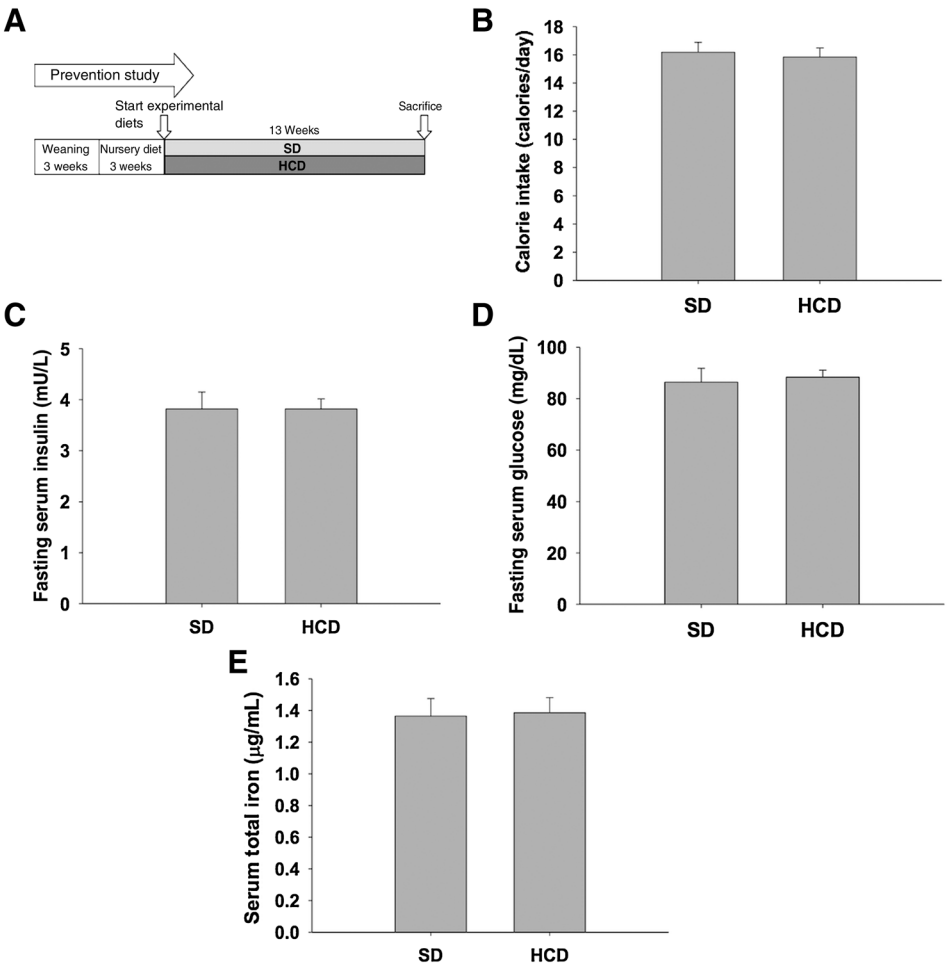


**Figure 1.**

**A,** Study design: after weaning, pigs were divided into two groups and fed HCD or SD for 13 weeks. HCD-consuming pigs had similar calorie intake (**B**), fasting serum levels of insulin (**C**), glucose (**D**), and iron (**E**) compared with SD-consuming pigs. Insulin was measured using a radioimmunoassay following the manufacturer's protocol (Millipore). Glucose was measured using a commercially available kit (Cayman). Serum iron levels were measured as described in Materials and Methods. Results are expressed as mean ± SE for 7 to 8 animals in each treatment group.



Downloaded from cancerpreventionresearch.aacrjournals.org on October 19, 2017. © 2017 American Association for Cancer Research.

Published OnlineFirst June 2, 2017; DOI: 10.1158/1940-6207.CAPR-17-0010



**Table 1.** Composition of diets used in the study

| Ingredients (% of diet weight) | SD | HCD |
|---|---|---|
| Corn | 75.75 | 56.39 |
| Soybean meal w/o hulls | 21 | 21 |
| L-Threonine | 0 | 0.05 |
| L-Lysine HCl | 0.15 | 0.2 |
| DL-Methionine | 0 | 0.06 |
| Total minerals | 0.15 | 0.15 |
| Salt | 0.32 | 0.32 |
| Vitamin mix | 0.03 | 0.03 |
| Poultry fat | 1 | 3 |
| Dry fat | 0 | 17.1 |
| Dicalcium Phosphate | 0.9 | 1 |
| Limestone | 0.7 | 0.7 |
| **Total** | **100** | **100** |
| Dry matter | 89.6 | 91.7 |
| Metabolizable energy (Mcal/Kg) | 3,388 | 4,278 |
| Crude protein | 16.4 | 14.9 |
| Lysine | 0.84 | 0.84 |
| Methionine | 0.5 | 0.5 |
| Tryptophan | 0.16 | 0.15 |
| Threonine | 0.52 | 0.52 |
| Fat | 4.7 | 23 |
| Calcium | 0.6 | 0.62 |
| Phosphorus available | 0.23 | 0.24 |
| Phosphorus total | 0.52 | 0.48 |

current exploratory study. Feed intake was measured weekly until the end of the study. The dietary composition of standard diet (SD) and HCD is mentioned in Table 1. Poultry fat consists of 32% saturated and 68% unsaturated fat, whereas the dry fat used in HCD consists of 41% saturated and 60% unsaturated fat. The vitamin levels in vitamin mix are listed in Supplementary Table S2. The plant-based sources, corn and soybean meal, were all obtained from the same source and batch.

### Serum insulin and glucose levels

Insulin was measured using a radioimmunoassay following the manufacturer's protocol (Millipore). Glucose was measured using a commercially available kit (Cayman) following standard recommended protocol. Both insulin and glucose were measured after a 12-hour fast at week 11 of the study.

### Serum total iron levels

Serum total iron was measured according to the procedure described previously using a kit from Ricca Chemical Company (16). In brief, nonhemolyzed serum samples were mixed with an equal volume of acid solution to precipitate protein and liberate protein-bound iron. After centrifugation at 6,200 g for 10 minutes, clear supernatants were collected and mixed with an equal volume of chromogen solution (1.5 mol/L ferrozine and 1.5 mol/L saturated sodium acetate). After 10-minute incubation at room temperature, the absorbance was measured at 562 nm.

### Colon tissue collection

The animals were euthanized at the end of the study using a captive bolt method. The distal colon was resected, and the mucosa was collected and stored at −80°C until further analysis. Separately, a part of the distal colon was cleaned with RNase-free PBS, cut into pieces of 1 cm, and fixed with 10% buffered formalin. Paraffin-embedded tissues were sectioned at 4 μm and mounted on silane-coated slides for further analysis.

### Hematoxylin and eosin staining

Deparaffinized slides were dipped in Harris hematoxylin (Thermo Fisher Scientific) for 1 minute and washed in water/acid alcohol (0.03% HCL in 70% ethanol). The slides were then dipped in eosin for 1 to 2 minutes and gradually dehydrated in increasing concentrations of ethanol (100–100–95–70 v/v). Mounting media (Polysciences Inc.) were applied before placing coverslips.

### Immunofluorescence staining

***Pretreatment of slides.*** Prior to staining, the paraffin was softened and the tissue specimens fixed additionally by baking the slides in an oven at 55°C for 20 minutes. Deparaffinization was performed with a clearing agent (CitriSolv, Fisherbrand) twice for 5 minutes and hydrated with decreasing concentrations of ethanol (100–100–95–70 v/v). For target retrieval, the slides were incubated in citrate buffer at pH 6 (1 mmol/L citric acid) at 95°C for 20 minutes. To quench autofluorescence from formalin residues, slides were pretreated with sodium borohydride (1 mg/mL) for 5 minutes. Pig sections were blocked with mouse IgG serum from the Mouse On Mouse Kit (Vector Laboratories) and avidin/biotin as per the manufacturer's instructions (Vector Laboratories). The sections were blocked with superblock (Thermo Fisher Scientific) and avidin/biotin.

***KI-67.*** KI-67 antibody staining was performed using a mouse anti-KI-67 (Novocastra) for 1 hour at 37°C. Biotinylated horse anti-mouse secondary antibody (Vector Laboratories) with streptavidin rhodamine was used. Mounting media with DAPI (Vector Laboratories) was used as a counterstain.

***ASCL-2 and BMI-1.*** ASCL-2 staining was performed at 4°C overnight using a rabbit anti-ASCL-2 antibody (Abcam). BMI-1 antibody staining was performed using a goat anti-BMI-1 (LSBio) at 4°C overnight. Biotinylated goat anti-rabbit secondary antibody and biotinylated horse anti-goat secondary antibody with streptavidin fluorescein were used for ASCL-2 and BMI-1, respectively. The antibodies for ASCL-2 and BMI-1 were epitope matched with the pig protein sequences from the NCBI database. In addition, negative controls were used to ensure there is no false-positive staining. Additional sample images of the staining can be seen in the Supplementary Information (Supplementary Fig. S1). As the antibodies used were originally developed for human tissue, we stained normal human colon tissue sections and observed similar staining patterns (Supplementary Fig. S2). Mounting media with DAPI (Vector Laboratories) was used as a counterstain. All images were taken using Olympus BX-63 microscope with cellSens software.

### Proliferative zone and index analysis

Only U-shaped longitudinally cut crypts with open lamina and base touching the muscularis mucosa were selected for assessing the yield and distribution of labeled cells along the crypt. Twenty to 25 crypts per animal were counted. The total number of immunoreactive nuclei as well as the total number of nuclei per crypt column was counted. The proliferation index was defined as the percentage-labeled cells of the total number of crypt column cells. To assess the distribution of the labeled cells, the proliferative zone was calculated as the number of cells from the base to the most upper labeled cell divided by the total number of cells in the column multiplied by 100.



Downloaded from cancerpreventionresearch.aacrjournals.org on October 19, 2017. © 2017 American Association for Cancer Research.

Published OnlineFirst June 2, 2017; DOI: 10.1158/1940-6207.CAPR-17-0010



### Stem cell zone analysis

Three nonserial sections per animal were used for stem cell zone analysis. ASCL-2 and BMI-1 were used as the marker for stem cells. We obtained epitope-matched antibodies for ASCL-2 and BMI-1 and developed a protocol for reliably staining the stem cells in the pig colon. Only U-shaped, longitudinally cut crypts with open lamina and base touching the muscularis mucosa were selected for assessing the yield and distribution of labeled cells along the crypt. The total number of immunoreactive nuclei and the total number of nuclei per crypt column were counted. To assess the distribution of the labeled cells, the stem cell zone was calculated ($n = 8$ crypts/animal) as the position of the cell from the base to the most upper-labeled cell divided by the total number of cells in the column multiplied by 100 (Supplementary Fig. S3). At least 50 crypts positive for stem cell(s) were counted per treatment (on an average, 5 crypts stained positive out of 15–20 "U"-shaped crypts per section).

### Statistical analysis

Completely randomized block design was used in this study. Individual pigs were the experimental unit. The statistical procedure - mixed procedure PROC MIXED in SAS software (SAS Institute) was used for analysis of the serum markers, stem cell zone, and proliferative index and zone. The results were expressed as means ± SE for each treatment.

### Gut bacterial sequencing

Genomic DNA was extracted using PowerSoil DNA Extraction Kit (Mo Bio) from pig distal digesta samples. The hypervariable region 4 of the 16S ribosomal RNA gene was then amplified and sequenced on an Illumina HiSeq platform, yielding 83,757,806 sequences across 1,151 samples (17). Operational taxonomic units (OTU) were picked with multiplexed and quality filtered reads using UCLUST OTU picking algorithm (18) against the 13_5 release of Greengenes (19) using updated 13_8 taxonomy strings. The reads that failed to match the reference database at 97% identity were discarded to increase the statistical power of downstream analysis; the OTU table was initially filtered to only include OTUs that were present in at least 20 samples with a minimum count of 100 sequences, and then rarefied at 22,000 sequences per sample. The OTU reads of each bacteria for each animal were correlated to the proliferative index and zone as well as stem cell zone (ASCL-2 and BMI-1) data of each animal using spearman correlation.

### Proteomics

Distal colon mucosal protein was extracted using Complete Mammalian Proteome Extraction Kit (Millipore). After protein extraction, 100 μg each of protein samples was reduced, alkylated, and double-trypsin digested. Dried peptides were reconstituted in 0.1% formic acid, and 20 μg of tryptic peptides was injected onto a Polaris 2-mm × 100 mm C18 RP column using UHPLC at 0.4 mL/minute flow rate. All the samples were analyzed in triplicates on a high flow LC/AJS-dual ion Funnel Q-TOF mass spectrometer using a 30-minute gradient. The LC/MS-MS data were searched against NCBInr *Sus scrofa* (pig) database using Spectrum Mill bioinformatics tool, and results were summarized at 1% FDR. As there is no protein pathway database for pig proteins, we converted the pig proteins to human equivalent proteins using NCBI genbank accession IDs. In addition, as the pigs were used as a model for human physiology, only proteins with human homologs were considered in the study.

### Proteomics correlations

The main analysis consisted of three steps: an exploratory analysis of the protein profile, identification of the proteins that are correlated with the treatment groups, and a correlation analysis between the selected pathways and the stem cell/colon epithelial cell kinetics.

First, the data were cleaned to remove inconsistencies. Proteins that were not detected in multiple technical replicates were removed from the data as spurious signatures. The exploratory analysis was performed on the cleaned data using multidimensional scaling and Ward hierarchical clustering. These unsupervised clustering methods showed that there were clear patterns in the data that corresponded to the dietary treatment groups (Supplementary Fig. S4). As the treatment correlated with the protein profile, the next stage of the analysis involved looking for the proteins responsible for the correlation between the observed protein data and the treatment groups.

Sparse partial least squares discriminant analysis (sPLS-DA) was used to identify the proteins responsible for the correlation between the overall protein data and the treatment groups. sPLS-DA is a regression-based method for supervised clustering that can also provide sparse feature selection. As our goal is to find a small subset of proteins that are related to the treatment groups, sPLS-DA is suitable for this analysis. As sPLS-DA uses a variable sparsity penalty, 10-fold cross-validation was used to determine the sparsity penalty. The resulting list of proteins related to the treatment groups was further analyzed using Ingenuity Pathway Analysis (IPA) to identify the chemical pathways that may be related to the treatment groups. Fisher exact test was used to calculate the *P* value, determining the probability that each canonical pathway assigned to this dataset was not due to chance alone.

For correlation analysis between the selected pathways and the stem cell/colon epithelial cell kinetics, a linear regression was performed to evaluate the association between the proteins in the identified pathways and the stem cell/colon epithelial cell kinetics. The adjusted $R^2$ values were calculated for each pathway. The significance of the adjusted $R^2$ values was confirmed using bootstrapping. The adjusted $R^2$ values for the IPA pathways were compared with the adjusted $R^2$ values for 10,000 randomly generated pathways. Only IPA pathways that had an adjusted $R^2$ greater than 95% of the randomly generated pathways were considered significant.

## Results

### Pigs consuming HCD had no change in total calorie intake, serum iron, insulin, and glucose

SD-consuming pigs had a higher feed intake than HCD-consuming pigs. This is likely because SD was a less energy-dense diet (Table 1), although the calorie intake was similar between the groups (Fig. 1B). Animals were fasted for 12 hours, and serum was collected to measure serum insulin/glucose. We did not observe any differences in serum iron, insulin, or glucose between SD- and HCD-consuming pigs (Fig. 1C–E). The bodyweight gain and feed intake over the period of the study were also similar between the treatment groups (Supplementary Table S1). The lack of significant differences between the SD- and HCD-fed pigs for above-mentioned parameters allowed us to compare the effect



Downloaded from cancerpreventionresearch.aacrjournals.org on October 19, 2017. © 2017 American Association for Cancer Research.

Published OnlineFirst June 2, 2017; DOI: 10.1158/1940-6207.CAPR-17-0010



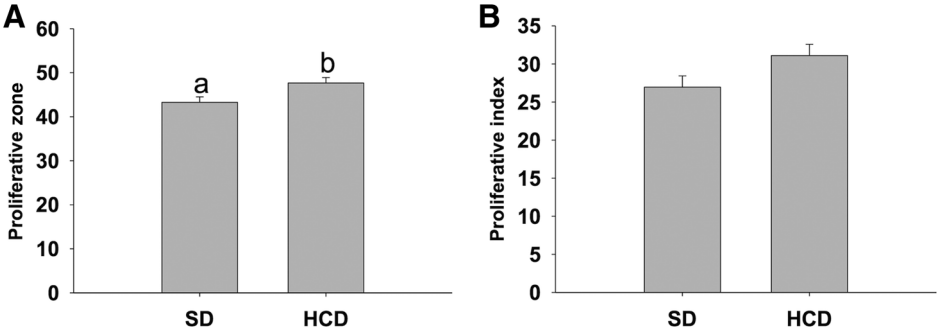


**Figure 2.**
HCD elevated proliferative zone (**A**) and proliferative index (**B**) in the pig colon crypt. Quantification was performed by immunofluorescence using proliferative marker KI-67. Results are expressed as mean ± SE for 7 to 8 animals in each treatment group. Means that differ by a common letter (a, b) differ ($P < 0.05$). At least 25 crypts per animal were analyzed.

of diet on colonic epithelial cells and bacteria independent of calorie intake, serum iron, insulin, and glucose levels.

### HCD elevated proliferative zone and index of colonic epithelial cells

HCD has been shown to increase the risk for colon cancer (20). A recent study showed the causal link between HCD and colon cancer (21). Proliferative zone and index in the crypt are elevated in colon cancer (22, 23); we measured both the proliferative zone and index in SD- and HCD-consuming pigs. HCD elevated proliferative zone significantly (Fig. 2A). There was a trend toward elevated proliferative index in HCD-consuming pigs compared with SD (Fig. 2B).

### HCD elevated stem cell zone

Colonic stem cells have been shown to be marked by various markers, such as LGR5/ASCL-2 (12) and BMI-1 (13). In addition, it was shown that ASCL-2 and BMI-1 stain different subsets of stem cells that are involved in extreme stress response (15). Hence, we used epitope-matched antibodies against ASCL-2 and BMI-1 to detect colonic stem cells in the colon crypts of the pigs (Fig. 3). The stem cell zone was calculated separately for ASCL-2 and BMI-1. The stem cell zone detected using ASCL-2 was significantly elevated (23%) in HCD-consuming pigs compared with SD (Fig. 3A and C). BMI-1 stem cell zone was also elevated in HCD-consuming pigs but was not significant (Fig. 3B and D).

### Proliferative zone and index highly correlated with innate inflammatory markers

We correlated the proliferative zone and proliferative index with inflammatory markers measured in the colonic mucosa (Supplementary Table S3) to understand the functional relevance of this elevation in proliferation to inflammation. Proliferative zone significantly correlated with inflammatory markers TLR-4, NF-κB, and IL6 (Table 2). Proliferative index significantly correlated with IL6. In addition, lipocalin-2 (LCN-2), a fecal

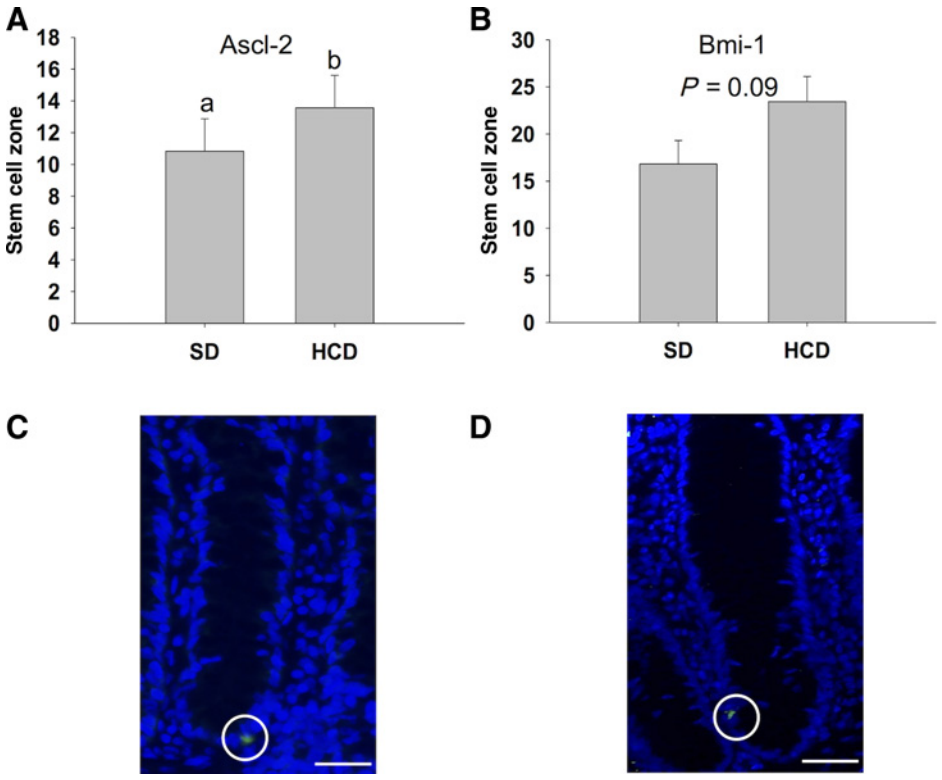


**Figure 3.**
HCD elevated stem cell zone in the pig colon crypt. Quantification was performed by immunofluorescence using ASCL-2 (**A**) and BMI-1 (**B**) stem cell marker for stem cell zone. Results are expressed as mean ± SE for 7 to 8 animals in each treatment group. Means that differ by a common letter (a, b) differ ($P < 0.05$). At least eight crypts per animal were analyzed. **C** and **D,** Stem cell marker ASCL-2 and BMI-1 were used to identify colonic stem cells, respectively. ASCL-2 and BMI-1 were detected at the base of the crypt and circled. DAPI (blue) was used as a nuclear counter stain. Images are at 20×. Scale bar, 50 μm.



Downloaded from cancerpreventionresearch.aacrjournals.org on October 19, 2017. © 2017 American Association for Cancer Research.

Published OnlineFirst June 2, 2017; DOI: 10.1158/1940-6207.CAPR-17-0010



**Table 2.** HCD-elevated proliferative zone and index highly correlated with elevated colonic inflammatory markers

| | Proliferative zone | Proliferative index | TLR-4 | NF-κB | IL6 | LCN-2 |
|---|---|---|---|---|---|---|
| Proliferative zone | N/A | 0.709[a] | 0.600[b] | 0.569[b] | 0.743[a] | 0.626[a] |
| Proliferative index | 0.709[a] | N/A | 0.121 | 0.099 | 0.604[b] | 0.319 |

[a]Significant at the 0.01 level.
[b]Significant at the 0.05 level.

inflammatory marker, was significantly elevated in the distal colon digesta of HCD-fed pigs and was significantly correlated with proliferative zone.

### HCD-induced alterations in bacteria correlated with proliferative and stem cell zone

Earlier studies have shown that HCD supplementation resulted in an altered abundance of the bacteroidetes and firmicutes phyla *in vivo* (24, 25). Studies in pigs have shown that lean cloned pigs contained relatively less bacteria belonging to the phylum firmicutes and more from the phylum bacteroidetes than obese cloned pigs. Proliferative index positively correlated with proteobacteria, while negatively correlated with firmicutes and bacteroidetes (Fig. 4). Proliferative zone positively correlated with firmicutes. Stem cell zone (ASCL-2) also positively correlated with proteobacteria and negatively correlated with firmicutes, which was increased in HCD scenario (Fig. 4). BMI-1 stem cell zone significantly correlated with bacterial changes compared with the other markers. BMI-1 stem cell zone positively correlated with proteobacteria and negatively correlated with a majority of firmicutes. Overall from the data, it is evident that stem cell zone (ASCL-2 and BMI-1) and proliferative index positively correlated with proteobacteria, which has been shown to be consistently elevated in high-fat diet/obesogenic conditions and inflammatory bowel diseases.

### Proteomics data and exploratory analysis reveals high correlation with pathways associated with colon cancer

Our analysis of distal colon mucosa using Jet Stream Proteomics revealed around 6,000 unique proteins, with about 4,000 being consistently detected over multiple runs (proteins that were not present in all the three replicates of at least one sample were considered to be artifacts and discarded for analysis). The accession numbers of the proteins that were significantly different were uploaded to IPA database to obtain the list of pathways. However, the list of pathways produced by IPA is based on the number of proteins present in the pathway. As proteins are either decreased/increased on the basis of their function or stimuli, the pathway list generated by IPA cannot be used to draw associations. Hence, we correlated the proteins in each of these pathways to our colonic epithelial cell kinetics parameters and generated rankings based on the strength of the correlations (described in Materials and Methods). This resulted in generating the top pathways with proteins that correlate with elevated colonic epithelial cell kinetics (Table 3). The top pathways that correlate with stem cell zone (ASCL-2 and BMI-1) are primarily involved in the migration/motility (Rho-GDI, Gap junction, FLT3) and proliferation (FAK, ERK/MAPK, eIF4). In addition, mTOR signaling pathway, which has been shown to alter stem cell proliferation in response to calorie changes (26), also correlated with stem cell zone. Similarly, proliferative zone and index correlated with pathways that

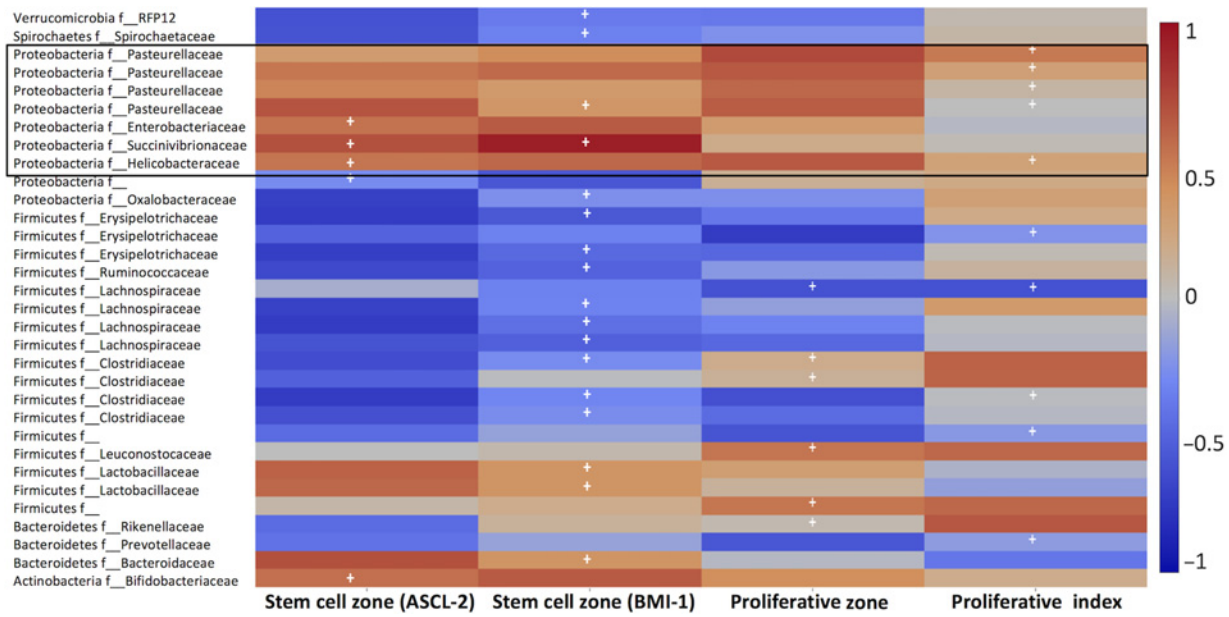


**Figure 4.**
Correlation heatmap between colonic phyla level bacteria to colonic epithelial cell kinetics. Significant correlations ($P < 0.05$) are shown with "+" sign. The scale bar on the right shows correlation value from "1 to −1." The bacteria are shown at phyla and family level.



Downloaded from cancerpreventionresearch.aacrjournals.org on October 19, 2017. © 2017 American Association for Cancer Research.

Published OnlineFirst June 2, 2017; DOI: 10.1158/1940-6207.CAPR-17-0010



**Table 3.** List of top altered pathways for stem cell zone, proliferative zone, and proliferative index

| Stem cell zone | Proliferative zone and index |
|---|---|
| Rho-GDI signaling | Role of tissue factor in cancer |
| FLT3 signaling in hematopoietic progenitor cells | Breast cancer regulation by Stathmin1 |
| Breast cancer regulation by Stathmin1 | Gap junction signaling |
| ERK/MAPK signaling | Glucocorticoid receptor signaling |
| mTOR signaling | Actin cytoskeleton signaling |
| FAK signaling | RAC signaling |
| Regulation of eIF4 and p70S6K signaling | FLT3 signaling in hematopoietic progenitor cells |
| Gap junction signaling | Neuregulin signaling |
| Semaphorin signaling in neurons | Regulation of IL2 expression in activated and anergic T lymphocytes |
| STAT3 pathway | CDC42 signaling |

are involved in cancer progression (tissue factor, breast cancer regulation by Stathmin1), migration/motility (actin cytoskeleton, FL3), and proliferation (RAC, neuregulinm and CDC42) along with glucocorticoid receptor signaling that is involved in T-cell activation (27).

## Discussion

In this study, we demonstrate that HCD drives the expansion of colonic stem cell zone and proliferative zone before the onset of dysregulated glucose metabolism and weight gain in a human-relevant pig model. The expansion of the colonic stem cell zone and proliferative zone may be due to the altered gut bacterial signature and elevated inflammation, which is supported by strong correlations.

Previous evidence has shown that proliferative cell numbers in the crypt are elevated in colon cancer (28). Furthermore, recent evidence has shown that HCD elevated intestinal stem cell numbers and their proliferative function *ex vivo* (2). As HCD has a causal link to colon cancer (20), we measured both the stem cell zone and proliferative zone in SD- and HCD-consuming pigs. SD-consuming pigs had higher food intake, but the overall calorie intake was similar between the two groups. HCD consumption in pigs had similar levels of total calorie intake, serum iron, insulin, and glucose compared with SD (Fig. 1B–E). This allowed us to look at the impact of HCD intake in the absence of metabolic dysfunction, such as glucose intolerance, hypoferremia, and weight gain. This is particularly significant because recent research has shown that HCD first affects the intestine in the form of altered gut bacterial changes and permeability, which can eventually lead to glucose intolerance (29).

HCD significantly elevated both ASCL-2 stem cell zone and proliferative zone (Figs. 2 and 3). We have developed a simple and specific immunofluorescence assay for the detection of stem cells in the pig colon crypts and thus were able to assess the effect of HCD on colonic stem cells in a human-relevant animal model. The assay employs epitope-matched antibodies and optimized incubation times for antibody staining to specifically detect stem cells using two different markers, ASCL-2 and BMI-1 (Fig. 3). ASCL-2–positive stem cells have been shown to participate in regular homeostasis, and its increase was corresponding to the increase in the proliferative zone. BMI-1 stem cell zone increase was not significant; this can be attributed to the fact that earlier studies have shown that BMI-1–positive stem cells are quiescent and activated in extreme stress, such as radiation exposure in mice (15). Unlike mice, pig gastrointestinal tract is anatomically and physiologically more similar to humans than any other nonprimate mammals. For example, BMI-1 stem cell population is not present in mouse colon (30), but here, we show that pig does contain BMI-1 population of stem cells similar to that of human colon (31). The increase in stem cell zone and the proliferative zone was independent of calorie intake, and before the onset of glucose intolerance, thus indicating that HCD consumption alone can cause an increase in stem cell zone and proliferative zone.

HCD-induced alterations in colonic bacteria and activation of Toll-like receptor (TLR) are key elements in the induction of the innate inflammatory response via triggering signaling cascades, including the transcription factor NF-κB (9, 32). Furthermore, high amounts of saturated fatty acids present in high-fat diets can directly activate TLR/NF-κB–mediated proinflammatory signaling pathways (33, 34). HCD-consuming pigs had elevated levels of inflammatory markers TLR-4 and NF-κB (Supplementary Table S3). Proliferative zone significantly correlated with innate inflammatory markers TLR-4 and NF-κB (Table 2), indicating that innate inflammation has an effect on proliferative kinetics of colonic epithelial cells. Recent research has shown that NF-κB plays a role in epithelial cell proliferation by increasing nuclear β-catenin accumulation upon exposure to innate inflammation, such as in colitis (35). Our strong correlation of proliferative zone to innate inflammatory markers further lends support to how an HCD diet can elevate the risk for colon cancer. LCN-2 is a stable and noninvasive marker of intestinal inflammation, which is secreted by both immune cells (primarily neutrophils) and colonic epithelial cells (36). LCN-2 expression is induced upon activation of TLRs on immune cells. HCD-consuming pigs had elevated levels of LCN-2 (Supplementary Table S3). Proliferative zone significantly correlated with LCN-2 measured in the colonic mucosa (Table 2), thus indicating that inflammation-induced stress elevates proliferation in colon epithelial cells. In addition, proliferative zone correlated positively with inflammatory marker IL6 (Table 2). IL6 was shown to be a critical promoter of epithelial cell proliferation in mice models of colitis-associated cancer (37). Furthermore, IL6 has been shown to mediate hypoferremia (iron deficiency). However, HCD-consuming pigs in our study did not have differences in serum iron levels compared with SD-consuming pigs (Fig. 1E). This can be probably explained by the low-grade chronic inflammation induced by HCD and thus allowing us to observe the effect of inflammation on colon kinetics without any systemic changes in the iron levels. The lack of stem cell zone correlations to inflammatory markers could be attributed to the asymmetric division of stem cells. Colonic stem cells divide asymmetrically to give rise to a daughter stem cell and a progenitor cell (38). Progenitor cells proliferate multiple times and differentiate into the various subtypes of colon epithelial cells, hence the strong correlation between proliferative index/zone (which accounts for all the proliferating cells) to inflammatory markers.

The colonic microbiota is estimated to comprise over $10^{14}$ bacteria from more than 1,000 different species. The results of the human microbiome project (39) by the NIH (Bethesda, MD) described more than 70 bacterial phyla, with four constituting the majority of mammalian microbiota (bacteroidetes, firmicutes, actinobacteria, and proteobacteria). In this study, we were able to test the relevance of these changes to host colonic epithelial cell kinetics. Stem cell zone and proliferative index positively



Downloaded from cancerpreventionresearch.aacrjournals.org on October 19, 2017. © 2017 American Association for Cancer Research.

Published OnlineFirst June 2, 2017; DOI: 10.1158/1940-6207.CAPR-17-0010



correlated with an increase in proteobacteria phylum, which has been associated with colitis and colorectal cancer (40). *E. coli*, a member of *Enterobacteriaceae* family/proteobacteria phylum, has been shown to produce colibactin, a genotoxin responsible for the promotion of colon cancer in chronic inflammatory mice models (40). HCD consumption is marked by a decrease in butyrate-producing bacteria (like *Clostridia*, which are part of the firmicutes phyla) and increase in proteobacteria. Proteobacteria lineages with more genes for signal transduction, cell migration/motility, and membrane transport are increased in abundance on the high-fat diet (41). Thus, the correlation of colonic epithelial cell kinetics with inflammation and proteobacteria indicates a potential role of gut bacteria in HCD-elevated colon cancer risk.

Correlation ranking of proteomic pathways revealed an association with pathways that are involved in proliferation, cell junction, and cytoskeleton signaling (migration/motility) and inflammation. FAK, ERK/MAPK, eIF4, and mTOR are pathways involved in increased proliferation that correlated with stem cell zone (Table 3). Mitogen-activated protein kinase (ERK/MAPK) and rapamycin-sensitive mTORC1 pathways are evolutionarily conserved kinase modules that link extracellular signals to fundamental cellular processes, such as growth, proliferation, differentiation, migration, and apoptosis (42). Recently, calorie alterations in animals have been shown to cause an increase in stem cell proliferation (43). eIF4 is involved in translation upregulation in the presence of growth factors (which are elevated in HCD-consuming animals; ref. 44). Actin cytoskeleton provides a supportive framework to the three-dimensional structure of cells and enables the cell to adopt a variety of shapes and to undertake directed movements. The correlation of this pathway to proliferative zone and index provides substantial basis for migration of proliferating cells across the colon crypt. This is particularly important in chronic inflammatory conditions, as migration across the crypt column leads to elevated exposure to intestinal luminal toxins, resulting in a greater chance of acquiring mutations while proliferating. Gap junction signaling is critically important in regulating tissue homeostasis, apoptosis, metabolic transport, and normal cell growth and differentiation (45). Junction dynamics are affected by cytokines like TNFα, which was elevated in our study and other chronic inflammatory conditions. In addition, the cytokine and growth factor–activated signaling pathways, STAT3 and IL2, correlated with stem cell zone, proliferative index, and proliferative zone, respectively. Collectively, this shows that the enhanced presence of growth factors and inflammation in HCD conditions can cause these alterations in gap junction signaling, which leads to altered colonic epithelial cell kinetics.

On the basis of the data, we can conclude that pigs contain both types of colonic stems cells (ASCL-2 and BMI-1; mice colon lacks BMI-1–type stem cells) similar to human and the HCD-induced changes in gut bacterial composition and elevated inflammation can result in stress to the colon epithelium, leading to elevated proliferative zone and index and stem cell zone. These changes are independent of calorie intake, body weight, and serum iron levels and before the onset of glucose intolerance. This elevation is further reflected in the colon epithelial proteome, high correlation to proliferation and motility pathways. Proliferating colonocytes are highly susceptible to toxicants from sources such as gut bacteria and diet. This is particularly important as up to 85% of the colon cancer cases are attributed to diet and lifestyle factors. Given that pig has distinct colonic stem cell population and gut bacterial profile similar to humans, the pig model can be utilized in the development of preventive and therapeutic agents/strategies against gut bacterial dysbiosis and inflammation-promoted diseases, such as colon cancer and type II diabetes.

## Disclosure of Potential Conflicts of Interest

No potential conflicts of interest were disclosed.

## Authors' Contributions

**Conception and design:** L. Reddivari, S.W. Kim, R. Knight, J.K.P. Vanamala
**Development of methodology:** V. Charepalli, L. Reddivari, J.K.P. Vanamala
**Acquisition of data (provided animals, acquired and managed patients, provided facilities, etc.):** V. Charepalli, L. Reddivari, S. Radhakrishnan, X. Xiao, S.W. Kim, V.B. Bhat, J.K.P. Vanamala
**Analysis and interpretation of data (e.g., statistical analysis, biostatistics, computational analysis):** V. Charepalli, L. Reddivari, S. Radhakrishnan, E. Eriksson, S.W. Kim, F. Shen, Q. Li, V.B. Bhat, R. Knight, J.K.P. Vanamala
**Writing, review, and/or revision of the manuscript:** V. Charepalli, L. Reddivari, F. Shen, M. Vijay-Kumar, R. Knight, J.K.P. Vanamala
**Administrative, technical, or material support (i.e., reporting or organizing data, constructing databases):** V. Charepalli, F. Shen, R. Knight, J.K.P. Vanamala
**Study supervision:** L. Reddivari, S.W. Kim, J.K.P. Vanamala

## Acknowledgments

We thank members of S.W. Kim's laboratory at North Carolina State University for their assistance with the pig study. We appreciate the help for the pig studies provided by members of the North Carolina State University Swine Education Unit, Raleigh, NC, Swine Evaluation Unit, Clayton, NC, and North Carolina State University Feed Mill, Raleigh, NC. Abigail Sido measured IL6 expression under the supervision of J.K.P. Vanamala, and these data were used for correlations performed in this study. We would also like to thank Dr. Na Xiong from Pennsylvania State University for providing thoughtful feedback on the manuscript draft.

## Grant Support

J.K.P. Vanamala is the principal investigator of USDA-NIFA NRI integrated grant 2009-55200-05197 that supported this work. L. Reddivari was partially supported by USDA-NIFA grant 2016-67017-24512 Gut bacterial analysis was partially funded by HHMI Early Career Scientist (awarded to R. Knight). Q. Li was partially supported by NIHR01GM109453 and 1UL1RR033184-01.

The costs of publication of this article were defrayed in part by the payment of page charges. This article must therefore be hereby marked *advertisement* in accordance with 18 U.S.C. Section 1734 solely to indicate this fact.

Received January 11, 2017; revised April 10, 2017; accepted May 30, 2017; published OnlineFirst June 2, 2017.

## References

1. Barker N. Adult intestinal stem cells: critical drivers of epithelial homeostasis and regeneration. Nat Rev Mol Cell Biol 2014;15:19–33.
2. Beyaz S, Mana MD, Roper J, Kedrin D, Saadatpour A, Hong S-J, et al. High-fat diet enhances stemness and tumorigenicity of intestinal progenitors. Nature 2016;531:53–8.



Downloaded from cancerpreventionresearch.aacrjournals.org on October 19, 2017. © 2017 American Association for Cancer Research.

Published OnlineFirst June 2, 2017; DOI: 10.1158/1940-6207.CAPR-17-0010




3. Reuter S, Gupta SC, Chaturvedi MM, Aggarwal BB. Oxidative stress, inflammation, and cancer: how are they linked? Free Radic Biol Med 2010;49:1603–16.
4. Lonkar P, Dedon PC. Reactive species and DNA damage in chronic inflammation: reconciling chemical mechanisms and biological fates. Int J Cancer 2011;128:1999–2009.
5. Martinez-Montiel Mdel P, Gomez-Gomez GJ, Flores AI. Therapy with stem cells in inflammatory bowel disease. World J Gastroenterol 2014;20: 1211–27.
6. Winzell MS, Ahrén B. The high-fat diet–fed mouse a model for studying mechanisms and treatment of impaired glucose tolerance and type 2 diabetes. Diabetes 2004;53:S215–S9.
7. Day SD, Enos RT, McClellan JL, Steiner J, Velázquez KT, Murphy E. Linking inflammation to tumorigenesis in a mouse model of high-fat-diet-enhanced colon cancer. Cytokine 2013;64:454–62.
8. Centers for Disease Control and Prevention. National diabetes statistics report: estimates of diabetes and its burden in the United States, 2014. Atlanta, GA: U.S. Department of Health and Human Services; 2014.
9. Li H, Lelliott C, Hakansson P, Ploj K, Tuneld A, Verolin-Johansson M, et al. Intestinal, adipose, and liver inflammation in diet-induced obese mice. Metabolism 2008;57:1704–10.
10. Kim KA, Gu W, Lee IA, Joh EH, Kim DH. High fat diet-induced gut microbiota exacerbates inflammation and obesity in mice via the TLR4 signaling pathway. PLoS One 2012;7:e47713.
11. Winer DA, Luck H, Tsai S, Winer S. The intestinal immune system in obesity and insulin resistance. Cell Metab 2016;23:413–26.
12. van der Flier LG, van Gijn ME, Hatzis P, Kujala P, Haegebarth A, Stange DE, et al. Transcription factor achaete scute-like 2 controls intestinal stem cell fate. Cell 2009;136:903–12.
13. Sangiorgi E, Capecchi MR. Bmi1 is expressed in vivo in intestinal stem cells. Nat Genet 2008;40:915–20.
14. Barker N, van Es JH, Kuipers J, Kujala P, van den Born M, Cozijnsen M, et al. Identification of stem cells in small intestine and colon by marker gene Lgr5. Nature 2007;449:1003–7.
15. Yan KS, Chia LA, Li X, Ootani A, Su J, Lee JY, et al. The intestinal stem cell markers Bmi1 and Lgr5 identify two functionally distinct populations. Proc Natl Acad Sci 2012;109:466–71.
16. Xiao X, San Yeoh B, Saha P, Olvera RA, Singh V, Vijay-Kumar M. Lipocalin 2 alleviates iron toxicity by facilitating hypoferremia of inflammation and limiting catalytic iron generation. Biometals 2016;29:451–65.
17. Caporaso JG, Lauber CL, Walters WA, Berg-Lyons D, Huntley J, Fierer N, et al. Ultra-high-throughput microbial community analysis on the Illumina HiSeq and MiSeq platforms. ISME J 2012;6:1621–4.
18. Edgar RC. Search and clustering orders of magnitude faster than BLAST. Bioinformatics 2010;26:2460–1.
19. DeSantis TZ, Hugenholtz P, Larsen N, Rojas M, Brodie EL, Keller K, et al. Greengenes, a chimera-checked 16S rRNA gene database and workbench compatible with ARB. Appl Environ Microbiol 2006;72: 5069–72.
20. Newmark HL, Yang K, Kurihara N, Fan K, Augenlicht LH, Lipkin M. Western-style diet-induced colonic tumors and their modulation by calcium and vitamin D in C57Bl/6 mice: a preclinical model for human sporadic colon cancer. Carcinogenesis 2009;30:88–92.
21. Vanamala J, Radhakrishnan S, Eriksson E, Charepalli V, Kim S, Reddivari L. High-fat diet induced expansion of colon crypt epithelial proliferative zone towards lumen correlates with elevated innate inflammatory markers in the human-relevant porcine model. FASEB J 2014;28:123.2.
22. Myant KB, Cammareri P, McGhee EJ, Ridgway RA, Huels DJ, Cordero JB, et al. ROS production and NF-kappaB activation triggered by RAC1 facilitate WNT-driven intestinal stem cell proliferation and colorectal cancer initiation. Cell Stem Cell 2013;12:761–73.
23. Zhang T, Otevrel T, Gao Z, Ehrlich SM, Fields JZ, Boman BM. Evidence that APC regulates survivin expression: a possible mechanism contributing to the stem cell origin of colon cancer. Cancer Res 2001;61:8664–7.
24. Ley RE, Bäckhed F, Turnbaugh P, Lozupone CA, Knight RD, Gordon JI. Obesity alters gut microbial ecology. Proc Natl Acad Sci U S A 2005; 102:11070–5.
25. Mujico JR, Baccan GC, Gheorghe A, Díaz LE, Marcos A. Changes in gut microbiota due to supplemented fatty acids in diet-induced obese mice. Br J Nutr 2013;110:711–20.
26. Harris TE, Thorner MO. Caloric restriction in mTORC1 control of intestinal homeostasis. Cell Metab 2012;16:6–8.
27. Cima I, Corazza N, Dick B, Fuhrer A, Herren S, Jakob S, et al. Intestinal epithelial cells synthesize glucocorticoids and regulate T cell activation. J Exp Med 2004;200:1635–46.
28. Bostick RM, Fosdick L, Grandits GA, Lillemoe T, Wood J, Grambsch P, et al. Colorectal epithelial cell proliferative kinetics and risk factors for colon cancer in sporadic adenoma patients. Cancer Epidemiol Biomarkers Prev 1997;6:1011–9.
29. Jensen BA, Nielsen TS, Fritzen AM, Holm JB, Fjære E, Serup AK, et al. Dietary fat drives whole-body insulin resistance and promotes intestinal inflammation independent of body weight gain. Metabolism 2016;65: 1706–19.
30. Tian H, Biehs B, Warming S, Leong KG, Rangell L, Klein OD, et al. A reserve stem cell population in small intestine renders Lgr5-positive cells dispensable. Nature 2011;478:255–9.
31. Kim JH, Yoon SY, Kim C-N, Joo JH, Moon SK, Choe IS, et al. The Bmi-1 oncoprotein is overexpressed in human colorectal cancer and correlates with the reduced p16INK4a/p14ARF proteins. Cancer Lett 2004;203: 217–24.
32. Takeda K, Akira S. TLR signaling pathways. Semin Immunol 2004;16:3–9.
33. Chait A, Kim F. Saturated fatty acids and inflammation: who pays the toll? Arterioscler Thromb Vasc Biol 2010;30:692–3.
34. Maury E, Brichard SM. Adipokine dysregulation, adipose tissue inflammation and metabolic syndrome. Mol Cell Endocrinol 2010;314:1–16.
35. Salcedo R, Worschech A, Cardone M, Jones Y, Gyulai Z, Dai R-M, et al. MyD88-mediated signaling prevents development of adenocarcinomas of the colon: role of interleukin 18. J Exp Med 2010;207:1625–36.
36. Chassaing B, Srinivasan G, Delgado MA, Young AN, Gewirtz AT, Vijay-Kumar M. Fecal lipocalin 2, a sensitive and broadly dynamic non-invasive biomarker for intestinal inflammation. PLoS One 2012;7:e44328.
37. Hu B, Elinav E, Huber S, Strowig T, Hao L, Hafemann A, et al. Microbiota-induced activation of epithelial IL-6 signaling links inflammasome-driven inflammation with transmissible cancer. Proc Natl Acad Sci U S A 2013; 110:9862–7.
38. Potten CS, Owen G, Booth D. Intestinal stem cells protect their genome by selective segregation of template DNA strands. J Cell Sci 2002;115:2381–8.
39. Peterson J, Garges S, Giovanni M, McInnes P, Wang L, Schloss JA, et al. The NIH human microbiome project. Genome Res 2009;19:2317–23.
40. Arthur JC, Perez-Chanona E, Mühlbauer M, Tomkovich S, Uronis JM, Fan T-J, et al. Intestinal inflammation targets cancer-inducing activity of the microbiota. Science 2012;338:120–3.
41. Hildebrandt MA, Hoffmann C, Sherrill-Mix SA, Keilbaugh SA, Hamady M, Chen YY, et al. High-fat diet determines the composition of the murine gut microbiome independently of obesity. Gastroenterology 2009;137: 1716–24.
42. Kim EK, Choi E-J. Pathological roles of MAPK signaling pathways in human diseases. Biochim Biophys Acta 2010;1802:396–405.
43. Laplante M, Sabatini DM. mTOR signaling in growth control and disease. Cell 2012;149:274–93.
44. Magnuson B, Ekim B, Fingar DC. Regulation and function of ribosomal protein S6 kinase (S6K) within mTOR signalling networks. Biochem J 2012;441:1–21.
45. Nicholson BJ. Gap junctions–from cell to molecule. J Cell Sci 2003; 116:4479–81.




Downloaded from cancerpreventionresearch.aacrjournals.org on October 19, 2017. © 2017 American Association for Cancer Research.

Published OnlineFirst June 2, 2017; DOI: 10.1158/1940-6207.CAPR-17-0010

AACR American Association for Cancer Research

Cancer Prevention Research

# Pigs, Unlike Mice, Have Two Distinct Colonic Stem Cell Populations Similar to Humans That Respond to High-Calorie Diet prior to Insulin Resistance

Venkata Charepalli, Lavanya Reddivari, Sridhar Radhakrishnan, et al.

*Cancer Prev Res* Published OnlineFirst June 2, 2017.

| | |
|---|---|
| **Updated version** | Access the most recent version of this article at: doi:10.1158/1940-6207.CAPR-17-0010 |
| **Supplementary Material** | Access the most recent supplemental material at: http://cancerpreventionresearch.aacrjournals.org/content/suppl/2017/06/02/1940-6207.CAPR-17-0010.DC1 |

| | |
|---|---|
| **E-mail alerts** | Sign up to receive free email-alerts related to this article or journal. |
| **Reprints and Subscriptions** | To order reprints of this article or to subscribe to the journal, contact the AACR Publications Department at pubs@aacr.org. |
| **Permissions** | To request permission to re-use all or part of this article, contact the AACR Publications Department at permissions@aacr.org. |

Downloaded from cancerpreventionresearch.aacrjournals.org on October 19, 2017. © 2017 American Association for Cancer Research.